Annales Societatis Geologorum Poloniae (2017), vol. 87: 41–53. doi: http://dx.doi.org/10.14241/asgp.2017.005

ELEMENTAL AND ORGANIC CARBON PROXIES FOR REDOX CONDITIONS OF THE OLIGOCENE FORMATIONS IN THE ROPA TECTONIC WINDOW (OUTER CARPATHIANS, POLAND): PALAEOENVIRONMENTAL IMPLICATIONS

Patrycja WÓJCIK-TABOL

Institute of Geological Sciences, Jagiellonian University, Gronostajowa 3a, PL-30-387, Kraków, Poland; e-mail: p.wojcik-tabol@ uj.edu.pl

Wójcik-Tabol, P., 2017. Elemental and organic carbon proxies for redox conditions of the Oligocene formations in the Ropa Tectonic Window (Outer Carpathians, Poland): palaeoenvironmental implications. *Annales Societatis Geologorum Poloniae,* 87: 41–53.

Abstract: The Oligocene Grybów Succession is recognized as a counterpart of the anoxic Menilite Formation. Its comprehensive geochemical investigations are made in the key sections of the Ropa Tectonic Window (the Grybów Unit, Polish Outer Carpathians). The maceral assemblages, dominated by land-plant liptinite, vitrinite and intertinite, correspond to kerogen types II and III. A T_{max} *vs.* HI diagram shows terrestrial kerogen type II with various additions of type III and algal kerogen type I. A variation in $\delta^{13}C_{org.}$ (from –25.21 to –27.38‰) may have resulted from variations in the composition of organic matter (the content of terrestrial *vs.* marine organic matter), controlled by depositional setting (turbidite *vs.* hemipelagic). The highest TOC contents are associated with an enhanced influx of land-derived organic matter. The redox-sensitive trace elements positively correlate with TOC and TS contents. Redox conditions varied between oxic and anoxic, as was concluded from TOC-TS, V/(V+Ni) and U/Th. The turbidity currents might have ventilated the bottom waters, especially more efficiently in the proximal zone of turbidite sedimentation. Moreover, oxygenated bottom waters may have also affected the concentration of trace metals, owing to migration of the redox interface downward within the sediments.

Key words: Organic matter, stable organic carbon isotope, trace metals, anoxia, Grybów Succession, Oligocene.

Manuscript received 11 December 2016 accepted 29 May 2017

INTRODUCTION

Near the Eocene-Oligocene boundary (EOB), the Earth's climate shifted towards cooler conditions. Changes in oceanic circulation, because of the opening of the Southern Ocean gateways (Kennett, 1977), a drop in atmospheric pCO_2 (DeConto and Pollard, 2003; Pagani *et al.*, 2005), and diminishing insolation (Coxall *et al.*, 2005), resulted in global cooling and the Antarctic glaciation (Diester-Haass, 1991; Zachos *et al.*, 1993; Liu *et al.*, 2009). A lowering sea level and limited water circulation led to O_2-poor conditions in the Early Oligocene Paratethys. The decrease in pCO_2 in the ocean-atmosphere system possibly was related to intensified weathering on the continent and accompanied organic carbon burial in the ocean. This climatic stress inhibited oceanic productivity, eventually causing a large-scale extinction (Prothero, 1994). The geochemical fingerprints of the EOB extinction have been discussed by many researchers (e.g., Asaro *et al.*, 1982; Sarkar *et al.*, 2003a, b).

The Oligocene, anoxic black shale facies in the Tethys/Paratethys region spread from the Alpine Molasse Basin throughout the Carpathian region to the Caspian Basin (Vetö, 1987; Vetö and Hetényi, 1991; Krhovský, 1995; Soták *et al.*, 2001; Popov *et al.*, 2004; Schultz *et al.*, 2005; Puglisi *et al.*, 2006; Sachsenhofer and Schulz, 2006).

The bituminous shales of the Menilite Formation represent one of the Oligocene black shales of the Paratethys commonly accepted as representing an anoxic environment (Vetö and Hetényi, 1991; Rospondek *et al.*, 1997; Köster *et al.*, 1998; Soták *et al.*, 2001; Kotarba and Koltun, 2006). The Oligocene Podgrybowskie Beds and the Grybów Marl Formation (also known as the Grybów Beds) of the Grybów Unit are recognized as a counterpart of the Menilite Formation. The Grybów Unit developed on the most southern slope of the Silesian Basin. Therefore, the Podgrybowskie Beds and the Grybów Marl Formation represent the more external facies by comparison with those of the Menilite Formation (Bieda *et al.*, 1963; Książkiewicz, 1977). A partial isolation of the Carpatho-Pannonian basins and climatic changes in the Early Oligocene (NP23 nannoplankton zone) resulted in the onset of estuarine circulation and then development of a stagnant regime (Black Sea model; Soták,

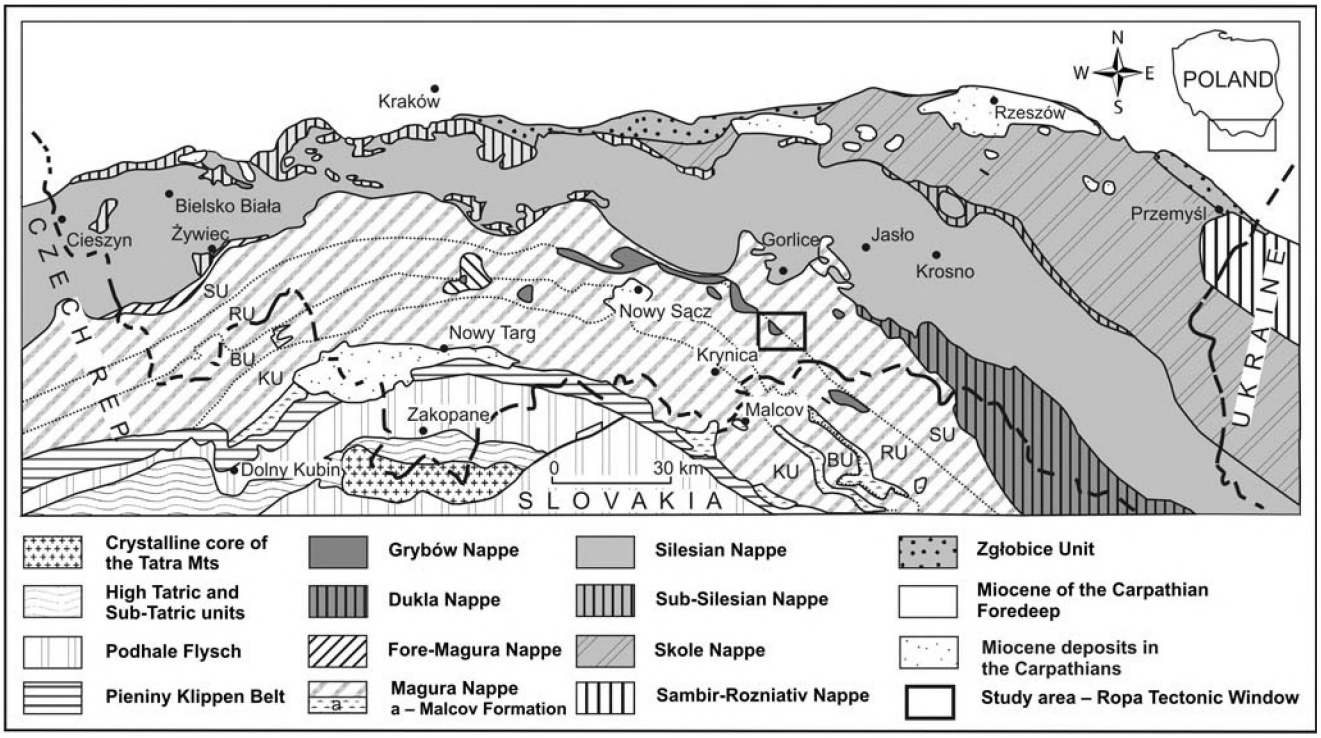

Fig. 1. Geological map of the central part of the Polish Carpathians, showing the location of the Ropa Tectonic Window (after Lexa *et al.*, 2000, modified); BU – Bystrica Unit, KU – Krynica Unit, RU – Rača Unit, SU – Siary Unit.

2008, 2010). However, Kotlarczyk *et al.* (2006) negated the commonly held view of estuarine circulation in the Carpathians Basin. Kotlarczyk and Uchman (2012) concluded that the depositional scenario of the black shales of the Menilite Formation to a limited extent can be referred to the Black Sea model. The water column was entirely anoxic only during a short period in the middle part of Rupelian, whereas the upper part of the formation was deposited in the basin with anoxia limited to the basin floor or to the upper slope; the latter situation may have been related to an oxygen-minimum zone, caused by upwelling events.

The depositional environment, including redox conditions, salinity and input of organic matter was studied in the Oligocene formations, using organic geochemistry (kerogen description and biomarkers), stable isotopes composition in carbonates ($\delta^{13}C_{carb.}$, $\delta^{18}O$) and in kerogen and hydrocarbons ($\delta^{13}C_{org.}$), sedimentological and microfacies analyses (e.g., Zachos *et al.*, 1996; Rospondek *et al.*, 1997; Köster *et al.*, 1998; Więcław, 2002; Sarkar *et al.*, 2003a, b; Kotarba and Koltun, 2006; Sachsenhofer *et al.*, 2009; Soták, 2010; Bechtel *et al.*, 2012; Bojanowski, 2012).

It is worth asking whether any such chemical records could be found in the Oligocene succession of the Grybów Unit. Wójcik-Tabol (2015) used such indices as U/Th, V/(V+Ni), Ni/Co, TOC, and TOC/S in an attempt to interpret the redox conditions of the Oligocene sediments of the Grybów Unit in the Grybów Tectonic Window.

In this paper, comprehensive geochemical investigations (stable carbon isotope ratio and major, and trace-elements variation, kerogen examination) of Oligocene sediments are reported for key sections of the Ropa Tectonic Window (Grybów Unit). The data sets obtained are compared to those of other Oligocene black shales of the Paratethys, known from the literature, to distinguish the different sedimentary environments of the basin.

GEOLOGICAL SETTING

The Fore-Magura Group of units, including the Grybów Unit (Świdziński, 1963), were formed in front of the Magura Nappe thrust. Deposits of the Grybów Unit are exposed only in tectonic windows in the Magura Nappe. Eleven tectonic windows of such affinity have been distinguished in the Polish part of the Magura Nappe (Fig. 1). The Grybów succession consists mainly of Late Eocene–Oligocene deposits (Sikora, 1960; Kozikowski, 1956; Oszczypko-Clowes and Oszczypko, 2004; Oszczypko-Clowes and Ślączka, 2006; Oszczypko-Clowes, 2008; Oszczypko and Oszczypko-Clowes, 2011), which starts with the Eocene Hieroglyphic Beds (Sikora, 1960, 1970), composed of greenish grey and dark grey shales, with intercalations of glauconitic sandstones. The Upper Eocene is represented by green marls, corresponding to the Globigerina Marl. This lithostratigraphic division is widespread and isochronous in all major units of the Outer Carpathians and the adjacent basins (Olszewska, 1983; Leszczyński, 1997).

The Oligocene sediments are developed as a series of 150 m-thick, greenish grey and brownish black, marly shales, intercalated with micaceous and glauconitic sandstones of the Podgrybowskie Beds (P-GBs; Kozikowski, 1956). They are overlain by the Grybów Marl Formation (GMF; Oszczypko-Clowes and Ślączka, 2006), which is also known as the Grybów Beds (Kozikowski, 1956). This for-

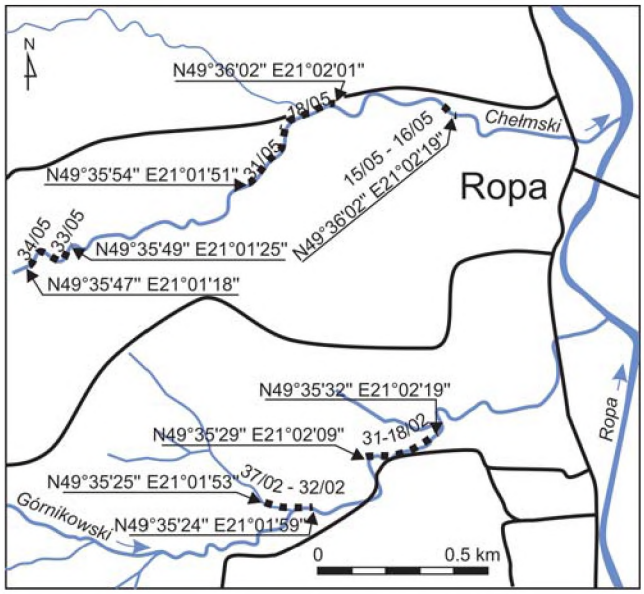

Fig. 2. Location of the sections studied; GPS coordinates of sampled parts of sections are given (after Oszczypko-Clowes *et al.*, 2015, simplified)

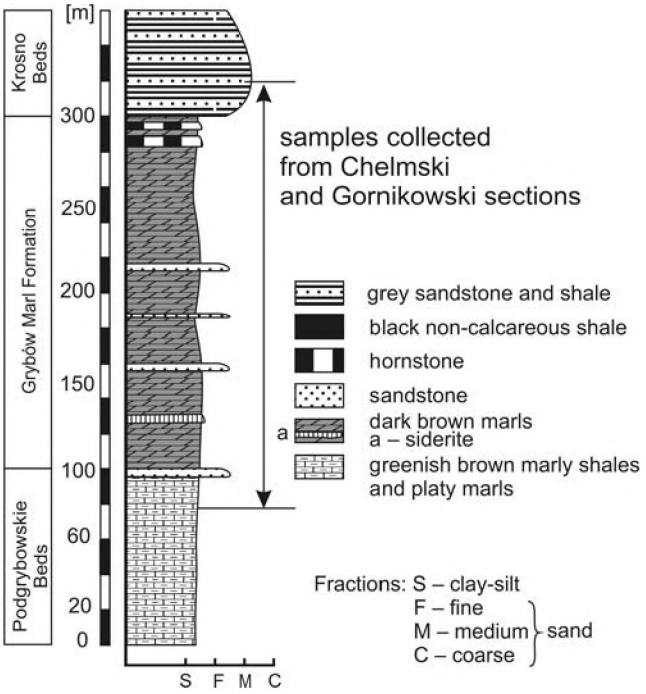

Fig. 3. Schematic lithostratigraphic column of the Grybów Succession in the Ropa Tectonic Window (modified after Sikora, 1970; Oszczypko-Clowes, 2008).

mation is up to 200 m thick. It occurs as a series of brownish black, platy-parting marls, with rare interbeds of grey marls and sandstones, and siliceous marls with cherts in the highest part of the formation. The youngest sediments of the Grybów Unit belong to the Krosno Beds (Kozikowski, 1956; Oszczypko-Clowes, 2008; Oszczypko and Oszczypko-Clowes, 2011), which are developed as a 400 m-thick series of grey, calcareous shales and micaceous sandstones. The biostratigraphical position of the series studied is the NP 24 nannoplankton zone (Oszczypko-Clowes, 2008).The Ropa Tectonic Window is located ca. 15 km SW of Gorlice (Fig. 1). It is up to 12 km long and 3 km wide. The investigations presented are focused on two sections, located on the northern slope of the Beskid Niski Range, along the Górnikowski and Chełmski creeks, which are left-bank tributaries of the Ropa River (Fig. 2). These sections were described by Kozikowski (1956), Sikora (1960, 1970), Ślączka (1973), Oszczypko-Clowes (2008) and Oszczypko-Clowes *et al.* (2015). The sections consist of strata referable to three thrust sheets.

MATERIALS AND METHODS

The samples were collected by Marta Oszczypko-Clowes during field work in 2002 and 2005. A sketch of lithostratigraphic column of the Ropa Tectonic Window is presented in Figure 3. The samples collected are shown in detail in Oszczypko-Clowes (2008, Fig. 3) and Oszczypko-Clowes *et al.* (2015, Fig. 3). They were taken from fine-grained sediments, including grey, green and brown mudstones and marls showing diverse carbonate content. The sections investigated were sampled continuously through the strata of three thrust sheets. They comprise a complete sequence from the Podgrybowskie Beds (11 samples) through the Grybów Marl Formation (16 samples) to the Krosno Beds (3 samples).

Organic petrology analysis was carried out on thirteen thin sections, using a Nikon-Eclipse 600 POL polarized (transmitted and reflected) light microscope, equipped with a mercury lamp, an excitation filter (EX 450–490 nm), dichroic mirror (DM 505 nm), and barrier filter (BA 520 nm) for investigations under blue UV light. The optical studies were conducted in the Institute of Geological Sciences of the Jagiellonian University.

The quantity of organic carbon (wt. % TOC) and type of kerogen were analysed in 15 samples of dark grey and brown marl and mudstone (five of Podgrybowskie Beds and ten of Grybów Marl Formation) by pyrolysis, using a Rock-Eval Model II instrument (for analytical details, see Espitalié *et al.*, 1985; Espitalié and Bordenave, 1993) at the Petrogeo Laboratory, Kraków.

Stable carbon isotopes were analysed for the organic matter of ten samples containing > 0.5 wt. % TOC. Before the carbon isotope analyses, the material was dried and washed with a 0.3M HCl solution in order to remove inorganic carbon phases. The material was combusted with CuO wire, under a vacuum at 900°C, using the sealed quartz tube method (Skrzypek and Jędrysek, 2005). The CO_2 obtained was cryogenically purified prior to transfer to a mass spectrometer. The analysis was conducted, using Finnigan Delta-V equipment. The $\delta^{13}C$ values were normalized to NBS-22 and USGS-24 international standards and then reported to the international Pee Dee Belemnite (VPDB) scale (Coplen *et al.*, 2006). The analytical precision was ±0.03‰. The isotopic analyses were performed by the Laboratory of Isotope Geology and Geoecology at Wrocław University. Thirty samples were chosen for geochemical studies. These samples represent a complete sequence from the Podgry-

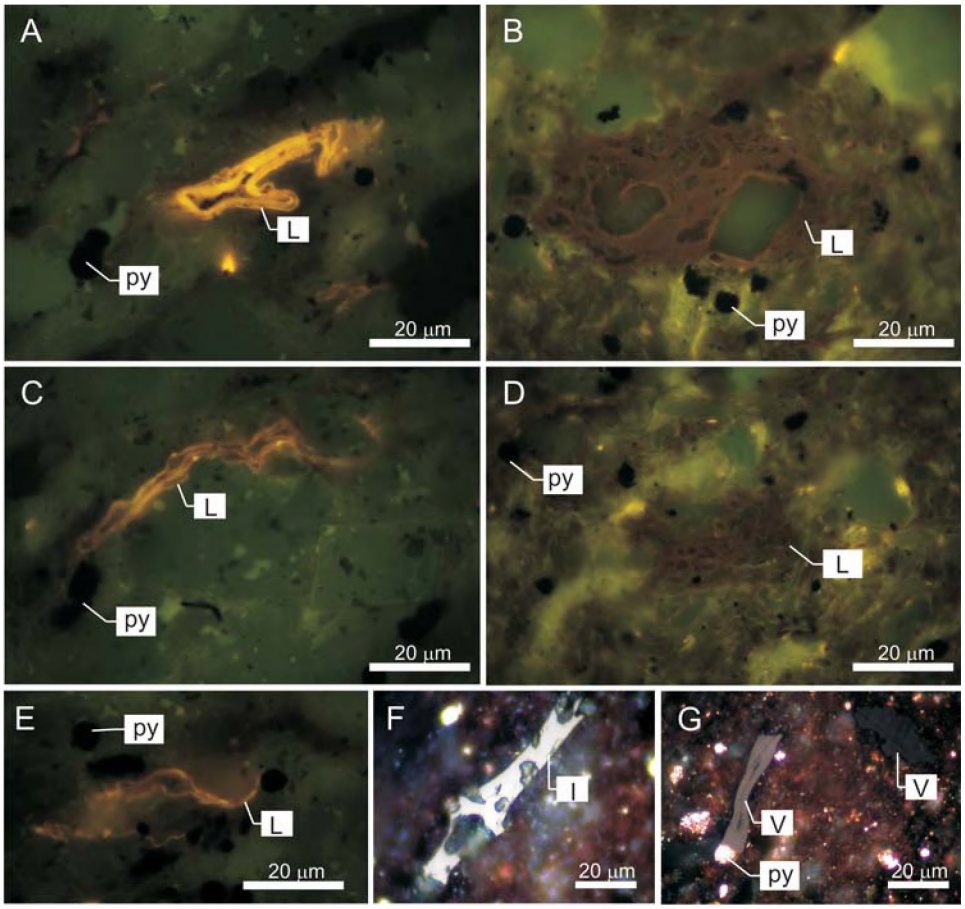

Fig. 4. Polarized light photomicroimages. A–E. Liptinite macerals and pyrite grains, UV blue illumination. F, G. Vitrinite and inertinite macerals and pyrite grains, reflected light; Py – pyrite, L – liptinite, V – vitrinite, I – inertinite.

bowskie Beds (eleven samples of marls and mudstones) through the Grybów Marl Formation (sixteen samples of marls and mudstones) to the Krosno Beds (two samples of mudstones and one sample of claystone). The rock samples were hand-pulverized in an agate mortar and pestle to the fraction passing 200 mesh. Sample amounts of typically 0.2 g dry weight pulp were decomposed by lithium borate fusion and dilute acid digestion before a classical whole-rock analysis by ICP emission spectrometry. Samples were analysed for eleven oxides (SiO_2, Al_2O_3, Fe_2O_3, MgO, CaO, Na_2O, K_2O, TiO_2, P_2O_5, MnO, Cr_2O_3) and loss on ignition (LOI), which is calculated from the weight difference after ignition at 1000 °C. Trace element contents were determined through the ICP-MS technique (ACME Analytical Laboratories, Ltd., 2013). A Leco device was used in total sulphur (TS) analysis (ACME Analytical Laboratories, Ltd., 2013). The amounts of major, minor and trace elements in the material studied were compared to those in the standard average shales (Wedepohl, 1971).

RESULTS

Organic petrography

An abundant maceral inventory was found in the dark grey and brown samples of the Podgrybowskie Beds and the Grybów Marl Formation. The assemblages are dominated by land-plant-derived macerals of the liptinite group, associated with minor amounts of vitrinite and intertinite.

The liptinite macerals, including sporinite, cutinite, resinite, and alginite (altered in bituminite) revealed orange brown and yellow luminescence in blue light (Fig. 4A–E). The green and grey samples contain only scarce black phytoclasts. The black debris is often structured (50–100 μm in diameter and elongated form up to 500 μm long) and shows white reflectance (Fig. 4F, G). It was defined as the macerals vitrinite and inertinite.

Organic matter is commonly accompanied by pyrite. In samples of the dark grey and dark brown marls, pyrite is abundant and adopts diverse forms, including numerous framboids, crystals, and massive lumps (Fig. 4). Their diameter ranges from 3 to 15 μm, from 5 to 10 μm, and up to 100 μm, respectively.

Rock-Eval pyrolysis indices

The Podgrybowskie Beds contain relatively low amounts of organic matter. Total organic carbon (TOC) content ranges from 0.18 to1.25 wt.%, with HI values varying between 62 and 146 mg HC/g TOC (Table 1). Values of T_{max} range from 436 to 445 °C and define kerogen type II and III on the T_{max} *versus* HI cross-plot (Fig. 5).

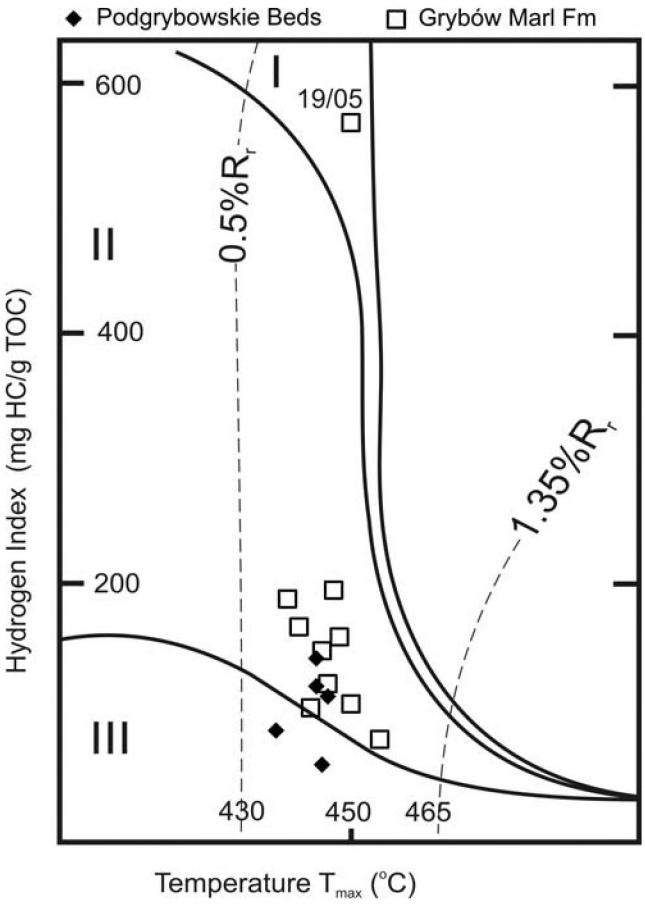

Fig. 5. Discriminant cross-plot of HI *vs.* T_{max} for organic maturity and kerogen type. Maturity paths of individual kerogen types after Espitalié *et al.* (1985); R_r – vitrinite reflectance scale.

The TOC contents of the Grybów Marl Formation are typically in the range of 0.15–2.3 wt. % with outliers at 4.86 and 5.68 wt. % TOC (Table 1). The highest values of TOC are found in brownish black marly shales in the Chełmski section. In contrast, low organic carbon contents (< 0.5 wt. % TOC) are obtained from grey and olive green samples of the Górnikowski section. T_{max} values are 438–454 °C. Diagram of T_{max} vs. HI shows that the samples represent mature (oil prone) kerogen type II with varying additions of type III. Kerogen type I is found only in one sample 19/05 (Fig. 5).

Stable isotope composition of organic matter

The $\delta^{13}C_{org}$ values range from –25.21 to –27.38 ‰ in the Podgrybowskie Beds and the Grybów Marl Formation (Table 1). The $\delta^{13}C_{org}$ values decrease from the Podgrybowskie Beds to the Grybów Marl Formation to –27.38 ‰ (sample 16/05) and rises afterward to –26.27 ‰ (sample 15/05). The upper part of the Grybów Marl Formation displays a positive $\delta^{13}C_{org.}$ excursion to -25.21 ‰ (sample 19/05), followed by a fall to –27.01 ‰ (sample 20/05). Generally, $\delta^{13}C_{org.}$ values become lower with rise of TOC and decrease of HI values in all samples (Fig. 6A, B).

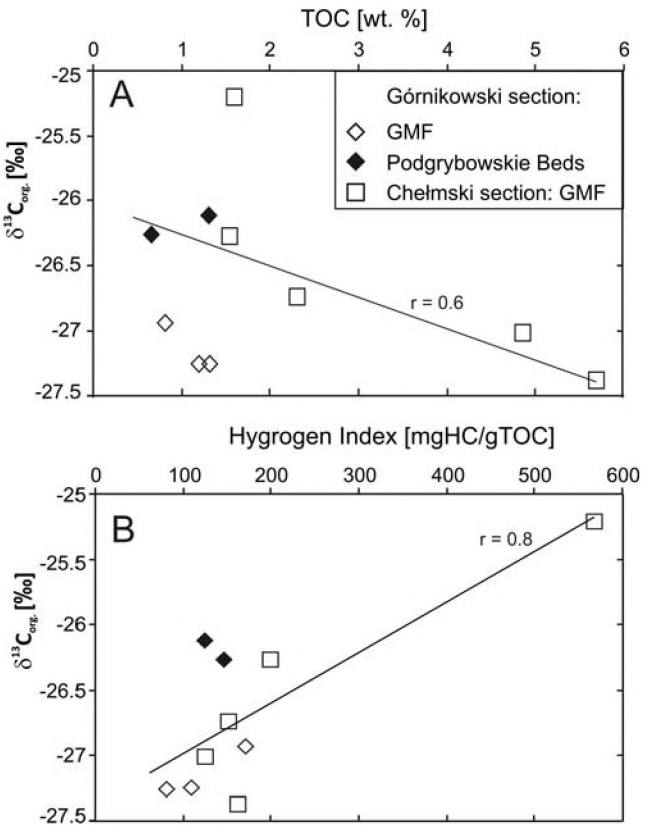

Fig. 6. Stable isotopic composition of the Grybów Unit samples. A. Correlation between $\delta^{13}C_{org.}$ and TOC. B. Diagram of $\delta^{13}C_{org.}$ *vs.* Hydrogen Index.

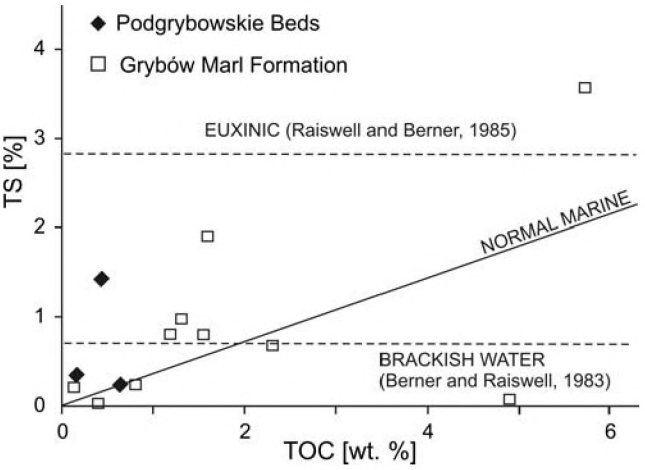

Fig. 7. Plot of TOC-rich samples of the Grybów Succession within the organic TOC *vs.* TS variation diagram.

Redox indicators

Carbon–sulphur relationships

Sulphate reduction, being coupled to the oxidation of sedimentary organic matter, can be expressed as TOC/TS ratios. TOC/TS in normal marine conditions is 2.8 ± 0.4. In contrast, values of TOC/TS > 2.8 are believed to indicate a brackish condition, whereas significantly lower TOC/TS values possibly reflect sulphate reduction (Berner and Rais-

Table 1

Chemical composition, Rock-Eval pyrolysis data and stable isotopic composition ($\delta^{13}C_{org.}$ of organic matter) for samples from the sedimentary succession of the Grybów Unit studied

				Górnikowski II															Górnikowski III		
				Podgrybowskie Beds									Grybów Marl Formation					Krosno Beds	Grybów Marl Formation		
	Unit	MDL	stan-dards	R15/02	R16/02	18/02	19/02	20/02	21/02	22/02	23/02	24/02	25/02	26/02	27/02	28/02	31/02	32/02	35/02	36/02	37/02
			STD SO-18; (1) STD DS8; (2) STD CSC	brown lamina-ted mud-stone	light brown lamina-ted mud-stone	green soft mud-stone	grey platy marl	ight brown lamina-ted mud-stone	greyish green soft marl (marly shale)	green soft marl	brown platy marl (marly shale)	yello-wish mud-stone	grey marl	green mud-stone	grey marl	light brown mud-stone	grey marl	grey mud-stone	green mud-stone	brown marl	brown mud-stone (marly shale)
SiO_2	%	0.01	58.11	n.d.	n.d.	52.36	38.37	57.43	43.85	41.62	36.96	46.92	38.71	41.75	39.29	43.65	36.06	42.13	44.54	36.92	42.77
Al_2O_3	%	0.01	14.09	n.d.	n.d.	15.83	10.54	13.18	13.66	13.51	12.83	13.17	12.86	13.76	12.07	15.42	13.07	12.15	14.07	13.12	12.54
Fe_2O_3	%	0.04	7.60	n.d.	n.d.	6.93	7.61	6.43	6.12	5.81	5.83	6.70	5.71	6.08	5.79	5.42	4.68	4.57	5.94	5.46	5.49
MgO	%	0.01	3.37	n.d.	n.d.	3.27	2.43	2.12	2.94	2.90	2.32	3.03	2.36	2.80	2.93	2.12	1.65	3.94	3.48	2.16	2.21
CaO	%	0.01	6.31	n.d.	n.d.	5.73	19.30	6.46	13.46	15.53	19.62	11.48	18.76	14.75	18.14	12.92	20.32	15.24	11.92	19.45	16.54
Na_2O	%	0.01	3.71	n.d.	n.d.	0.99	0.45	1.25	0.80	0.80	0.68	1.38	0.76	0.79	0.90	0.83	0.53	0.66	0.90	0.63	0.98
K_2O	%	0.01	2.17	n.d.	n.d.	2.92	1.63	2.32	2.80	2.82	2.40	2.25	2.58	2.83	2.22	3.01	2.70	2.49	2.62	2.48	2.46
TiO_2	%	0.01	0.69	n.d.	n.d.	0.78	0.39	0.73	0.67	0.66	0.58	0.76	0.61	0.69	0.60	0.64	0.58	0.56	0.71	0.57	0.62
P_2O_5	%	0.01	0.83	n.d.	n.d.	0.12	0.08	0.08	0.12	0.11	0.12	0.14	0.10	0.14	0.17	0.10	0.06	0.11	0.15	0.12	0.13
MnO	%	0.01	0.40	n.d.	n.d.	0.25	0.26	0.18	0.17	0.14	0.18	0.11	0.10	0.13	0.23	0.09	0.08	0.08	0.18	0.13	0.09
Cr_2O_3	%	0.00	0.56	n.d.	n.d.	0.02	0.01	0.03	0.02	0.02	0.02	0.03	0.02	0.02	0.02	0.02	0.01	0.02	0.02	0.02	0.03
LOI	%	-5.10	1.90	n.d.	n.d.	10.60	18.70	9.60	15.20	15.90	18.20	13.80	17.20	16.10	17.4	15.60	20.00	17.90	15.30	18.70	15.90
Th	ppm	0.20	10.90	n.d.	n.d.	13.40	7.40	11.00	11.40	12.30	10.20	10.80	11.90	11.50	9.60	12.90	11.70	9.80	11.80	11.10	10.90
U	ppm	0.10	17.30	n.d.	n.d.	2.90	2.80	3.30	3.10	3.10	3.40	2.80	2.90	2.70	2.70	3.10	2.30	3.50	4.30	7.20	5.80
V	ppm	8	212	n.d.	n.d.	149	101	122	140	137	137	125	138	135	115	155	139	130	129	177	160
Mo	ppm	0.10	14 (1)	n.d.	n.d.	0.40	0.60	1.50	0.50	0.50	1.40	0.70	0.40	1.30	0.40	1.00	0.60	1.10	0.70	5.60	5.30
Ni	ppm	0.10	38.9 (1)	n.d.	n.d.	81.90	61.90	61.40	70.70	66.50	75.40	71.90	87.10	76.40	60.50	73.90	53.90	64.50	68.10	101.10	92.10
TS	%	0.02	4.16 (2)	n.d.	n.d.	n.d.	n.d.	0.36	0.07	0.04	0.25	n.d.	0.22	0.03	0.13	0.25	0.04	0.41	0.14	0.81	0.98
Mo/U				n.d.	n.d.	0.14	0.21	0.45	0.16	0.16	0.41	0.25	0.14	0.48	0.15	0.32	0.26	0.31	0.16	0.78	0.91
U/Th				n.d.	n.d.	0.22	0.38	0.30	0.27	0.25	0.33	0.26	0.24	0.23	0.28	0.24	0.20	0.36	0.36	0.65	0.53
V/(V+Ni)				n.d.	n.d.	0.65	0.62	0.67	0.66	0.67	0.65	0.63	0.61	0.64	0.66	0.68	0.72	0.67	0.65	0.64	0.63
TOC/TS				n.d.	n.d.	n.d.	n.d.	0.50	n.d.	n.d.	2.64	n.d.	0.68	n.d.	n.d.	3.28	10.25	n.d.	n.d.	1.47	1.34
Tmax	°C			443	436	n.d.	n.d.	445	n.d.	n.d.	443	n.d.	438	n.d.	n.d.	440	442	n.d.	n.d.	n.d.	n.d.
TOC	wt.%			1.25	0.19	n.d.	n.d.	0.18	n.d.	n.d.	0.66	n.d.	0.15	n.d.	n.d.	0.82	0.41	n.d.	n.d.	n.d.	n.d.
HI	mg HC/g TOC			124	89	n.d.	n.d.	116	n.d.	n.d.	146	n.d.	193	n.d.	n.d.	171	107	n.d.	n.d.	n.d.	n.d.
OI	mg CO_2/ g TOC			32	36	n.d.	n.d.	188	n.d.	n.d.	68	n.d.	60	n.d.	n.d.	31	85	n.d.	n.d.	n.d.	n.d.
$\delta^{13}C$ org.	‰			-26.10	n.d.	n.d.	n.d.	n.d.	n.d.	n.d.	-26.26	n.d.	n.d.	n.d.	n.d.	-26.94	n.d.	n.d.	n.d.	n.d.	n.d.

MDL – method detection limit; n.d. – no data, the sample was not analyzed

well, 1983). Under euxinic bottom water, bacterial sulphate reduction occurs both in the water column and the sediments (Raiswell and Berner, 1985). The calculated TOC/TS ratios for the Oligocene samples studied vary from 0.32 to 3.32 with two outliers at 10.25 and 54 (Table 1), indicating that conditions varied from brackish to euxinic. In the TOC-TS plots (Fig. 7), many samples are located within the field of "normal marine". Two samples (16/05, 19/05) from the Grybów Marl Formation are located in the anoxic-euxinic field and two others (31/02, 20/05) are S-depleted, which is typical for a brackish environment. The TOC/TS ratios could have been seriously affected by conditions both euxinic and brackish, as in the Black Sea today and probably in the Paratethys during NP23 time (e.g., Schultz *et al.*, 2005; Soták, 2010). Post-depositional processes, which probably were responsible for the formation of the euhedras and large framboids of pyrite and the diagenetic degradation of organic matter, also may have altered the TOC/TS ratios and caused underestimation of them.

Redox-sensitive trace elements (RSTE): U, Mo, V, Ni

The distributions of U, Mo, V and Ni normalised to Al are presented in diagrams (Fig. 8). In general, the concentrations of redox-sensitive trace elements in the Podgrybowskie Beds are fairly low. The only exception is sample 1/07. The amounts of redox-sensitive trace elements (RSTE) tend

Table 1 continued

				Chełmski I						Chełmski II						Chełmski III		
				Grybów Marl Formation					Krosno Beds	Podgrybowskie Beds				Grybów Marl Formation		Grybów Marl Formation	Krosno Beds	
	Unit	MDL	standards	16/05	15/05	18/05	19/05	20/05	21/05	1/07	24/05	26/05	28/05	30/05	31/05	33/05	34/05	av.sh
			STD SO-18; (1) STD DS8; (2) STD CSC	brown mudstone (marly shale)	brown marl	light brown mudstone (marly shale)	brownish black mudstone (marly shale)	brown mudstone	greenish grey mudstone (marly shale)	dark grey fissile mudstone	grey claystone	green platy marl	grey platy marl	brown marl (marly shale)	grey marl (marly shale)	green mudstone	grey spoty claystone	
SiO_2	%	0.01	58.11	35.76	28.18	39.44	37.33	50.51	45.91	62.87	58.21	39.28	40.18	41.60	38.90	46.19	54.89	58.90
Al_2O_3	%	0.01	14.09	11.92	9.24	13.16	12.26	12.33	13.06	8.10	18.68	13.62	13.45	13.19	13.76	13.57	21.91	16.70
Fe_2O_3	%	0.04	7.60	7.44	3.67	6.40	4.88	5.60	4.14	7.88	6.78	4.49	5.17	5.66	5.96	5.61	5.47	6.90
MgO	%	0.01	3.37	1.45	1.51	2.73	1.55	1.23	2.28	1.60	2.82	1.87	2.01	1.89	2.35	2.97	2.67	2.60
CaO	%	0.01	6.31	16.50	27.81	15.51	17.44	8.99	13.58	7.67	0.60	18.15	17.33	15.09	17.02	10.75	0.70	2.20
Na_2O	%	0.01	3.71	0.43	0.44	0.84	0.46	0.53	0.79	0.68	0.89	0.73	0.75	0.54	0.74	0.70	0.97	1.60
K_2O	%	0.01	2.17	2.12	1.75	2.52	2.17	2.40	2.67	1.26	3.76	2.87	2.76	2.70	2.71	2.79	5.03	3.60
TiO_2	%	0.01	0.69	0.55	0.38	0.63	0.61	0.57	0.67	0.66	0.83	0.58	0.59	0.58	0.60	0.64	0.94	0.78
P_2O_5	%	0.01	0.83	0.15	0.13	0.12	0.13	0.19	0.13	0.06	0.09	0.06	0.08	0.11	0.13	0.12	0.09	0.16
MnO	%	0.01	0.40	0.30	0.12	0.15	0.34	0.03	0.08	0.18	0.03	0.18	0.08	0.07	0.15	0.20	0.04	n.d.
Cr_2O_3	%	0.00	0.56	0.02	0.02	0.03	0.02	0.02	0.02	0.01	0.02	0.01	0.01	0.02	0.02	0.02	0.02	n.d.
LOI	%	-5.10	1.90	23.10	26.50	18.20	22.60	17.40	16.50	8.90	7.10	17.90	17.40	18.30	17.40	16.30	7.10	n.d.
Th	ppm	0.20	10.90	9.80	7.60	11.30	10.80	9.70	12.00	8.10	14.70	12.20	11.90	11.00	12.10	11.50	17.90	n.d.
U	ppm	0.10	17.30	15.50	7.40	7.20	9.90	8.20	4.00	4.30	2.80	2.10	2.20	5.30	2.40	6.10	3.40	3.70
V	ppm	8	212	377	190	168	189	223	122	85	177	130	137	176	148	182	204	130.00
Mo	ppm	0.10	14 (1)	13.60	7.70	4.80	9.80	4.80	0.90	3.40	0.40	0.20	0.20	1.80	0.40	5.20	0.10	1.00
Ni	ppm	0.10	38.9 (1)	125.80	70.30	101.20	105.20	56.30	42.00	116.00	92.50	47.20	48.10	71.70	85.40	66.10	41.10	68.00
TS	%	0.02	4.16 (2)	3.57	0.81	1.15	1.91	0.09	0.07	1.42	0.06	n.d.	0.08	0.69	0.13	0.48	n.d.	n.d.
Mo/U				0.88	1.04	0.67	0.99	0.59	0.23	0.79	0.14	0.10	0.09	0.34	0.17	0.85	0.03	0.27
U/Th				1.58	0.97	0.64	0.92	0.85	0.33	0.53	0.19	0.17	0.18	0.48	0.20	0.53	0.19	n.d.
V/(V+Ni)				0.75	0.73	0.62	0.64	0.80	0.74	0.42	0.66	0.73	0.74	0.71	0.63	0.73	0.83	0.66
TOC/TS				1.59	1.91	n.d.	0.83	54.00	n.d.	0.32	n.d.	n.d.	n.d.	3.33	n.d.	n.d.	n.d.	n.d.
Tmax	°C			447	446	n.d.	449	445	n.d.	444	n.d.	n.d.	n.d.	444	n.d.	n.d.	n.d.	n.d.
TOC	wt.%			5.68	1.55	n.d.	1.59	4.86	n.d.	0.45	n.d.	n.d.	n.d.	2.3	n.d.	n.d.	n.d.	n.d.
HI	mg HC/g TOC			163	200	n.d.	569	126	n.d.	62	n.d.	n.d.	n.d.	152	n.d.	n.d.	n.d.	n.d.
OI	mg CO_2/g TOC			14	30	n.d.	19	29	n.d.	111	n.d.	n.d.	n.d.	15	n.d.	n.d.	n.d.	n.d.
$\delta^{13}C$ org.	‰			-27.38	-26.27	n.d.	-25.21	-27.01	n.d.	n.d	n.d.	n.d.	n.d.	-26.75	n.d.	n.d.	n.d.	n.d.

to increase in the Grybów Marl Formation with a maximum in sample 16/05. The RSTE contents correlate positively with TOC and S. The Pearson correlation coefficient is between 0.69 and 0.89, except for Ni *vs*. TOC, which exhibits a much weaker correlation (0.22; Table 2). The dark grey and brownish black samples enriched in TOC and TS are also enriched in RSTE, whereas samples enriched only in TOC (28/02, 28/05 and 30/05, 20/05) are not enriched in Mo and Ni. This indicates that Ni and Mo are bound to sulphides rather than to organic matter. All of these trace metals show negative or no correlation with Al_2O_3 (Fig. 9; Table 2), which indicates their non-detrital contribution.

Mo/U varies from 0.03 to 1.04 in the samples studied. The V/(V+Ni) ratio ranges from 0.61 to 0.83. One outlier of 0.42 was estimated for sample 1/07 from the Podgrybowskie Beds. The U/Th ratios for the deposits studied range from 0.2 to 1, with one outlier (sample 16/05) at 1.6 (Table 1).

DISCUSSION

Organic matter contribution

The maceral composition of the dispersed organic matter indicates a huge terrestrial input in the sediments of the Grybów succession. However, some contribution of marine organic matter cannot be excluded for some pelagic sediments of the Grybów Marl Formation (e.g., samples 17/05, 19/05).

The liptinite, predominant in maceral assemblages of the samples studied, originated from waxes and resins of the

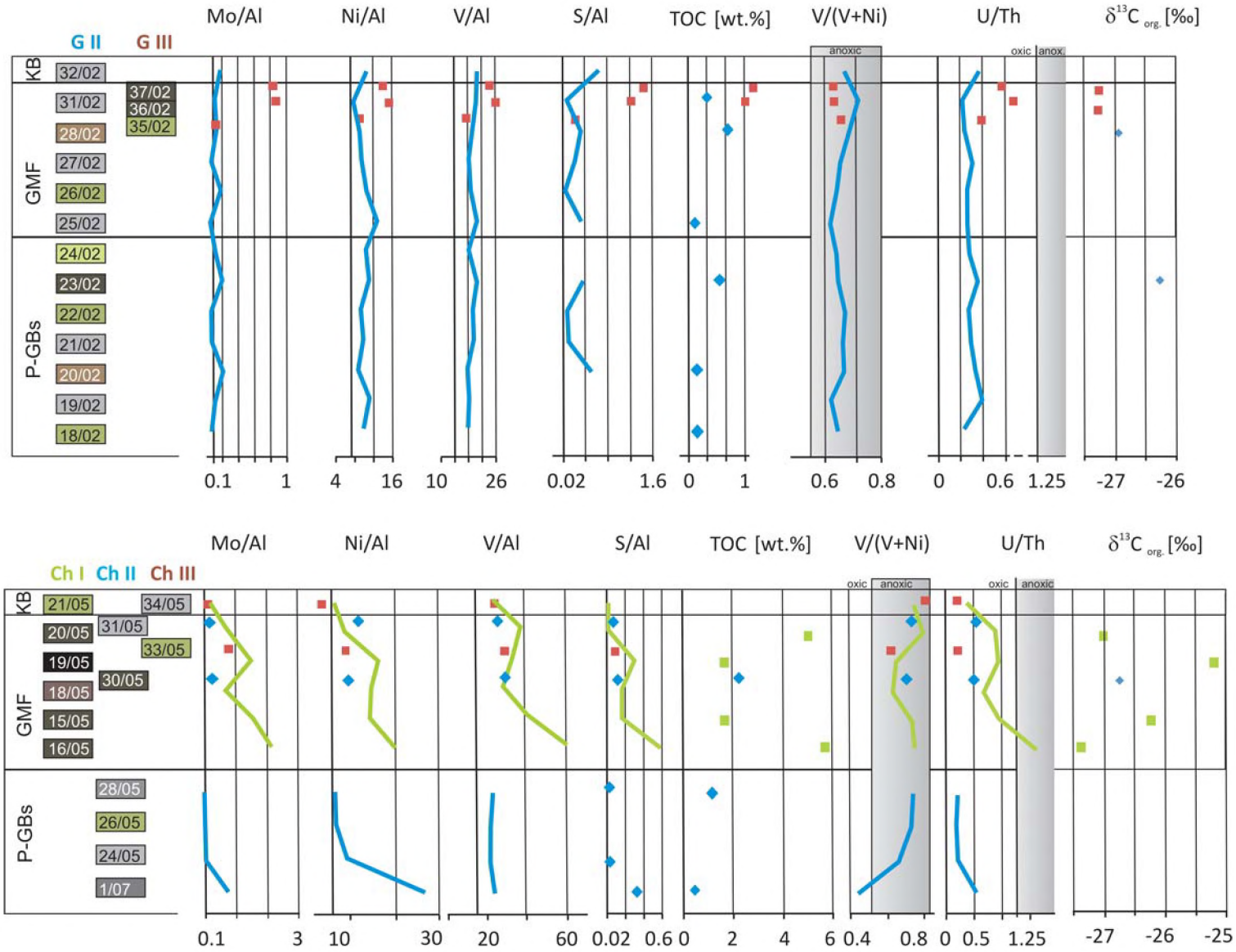

Fig. 8. Stratigraphic variation of redox geochemical proxies in the Oligocene strata studied. The patterns of distribution of Mo/Al, Ni/Al, V/Al, S/Al start from respective element/Al ratio for the average shales (after Wedepohl, 1971). The lines and points depict the element/Al for studied samples from continuous or discontinuous section. Their colour and section name are the same. GII, GIII – Górnikowski section, II and III thrust sheets; Ch I, Ch II, Ch III – Chełmski section, I, II and III thrust sheets; P-GBs – Podgrybowskie Beds, GMF – Grybów Marl Formation, KB – Krosno Beds. The colour of samples label shows the colour of sediment.

land plants admixed with zoo- and phytoplankton. They are the main components of kerogen types I and II (Peters and Moldowan, 1993). The black phytoclasts, defined as the macerals vitrinite and inertinite, are characterized by the high-C remnants of land plants. They are the chemical equivalents of type III and type IV of kerogen, respectively (Peters and Moldowan, 1993).

Pyrolysis data and the maceral assemblage correspond to isotope composition of $C_{org.}$. The variation in $\delta^{13}C_{org.}$ in the Grybów Unit sediments investigated is a function of supply of isotopically lighter terrigenous organic matter *versus* productivity pulses and varying amounts of autochthonous isotopically heavier organic matter (Meyers, 1994). The TOC peaks are correlated with an enrichment in ^{12}C, which indicates the enhanced supply of land-derived organic matter.

The $\delta^{13}C_{org.}$values of –27.38 ‰ associated with relatively low HI probably reflects the increasing terrestrial delivery of organic matter in the TOC-rich marly shales (sample 16/05). The later rise of $\delta^{13}C_{org.}$ to –26.27 ‰ occurs in the overlying brownish marls (sample 15/05). The enrichment of heavy carbon in the organic matter goes further up to the positive excursion ($\delta^{13}C_{org.}$ = –25.21 ‰) in the brow -nish black marly shales (sample 19/05). This positive excursion of $\delta^{13}C_{org.}$ is associated with high HI values, indicating some contribution of marine organic matter. The enrichment in ^{13}C could be a residual effect related to decreased terrestrial input, as it is accompanied by decreased TOC content and the subsequently enhanced presence of algal material that is isotopically heavier by comparison with freshwater organic matter (Meyers, 1994; Bechtel *et al.*, 2012). The burial of organic carbon in the ocean caused the $^{13}C_{org.}$ enrichment. The accelerated terrestrial input is recorded in the terminal fall in $\delta^{13}C_{org.}$ to –27.01 ‰, associated with a high TOC content and low HI in kerogen of the brownish calcareous mudstone (sample 20/05); this reveals a return to the predominance of terrigenous organic matter.

A similarly mixed contribution of terrestrial and marine organic matter was obtained from the Menilite Formation of the Outer Carpathians (Rospondek *et al.*, 1997; Köster *et al.*, 1998; Więcław, 2002; Kotarba and Koltun, 2006) and other Oligocene units, such as the Eggerding Formation in the Austrian Molasse Basin (Schulz *et al.*, 2002), the Ruslar Formation of the Kamchia Depression in the Eastern Paratthys, Bulgaria (Sachsenhofer *et al.*, 2009), and the Tard Clay of the Pannonian Basin in Hungary (Bechtel *et al.*, 2012).

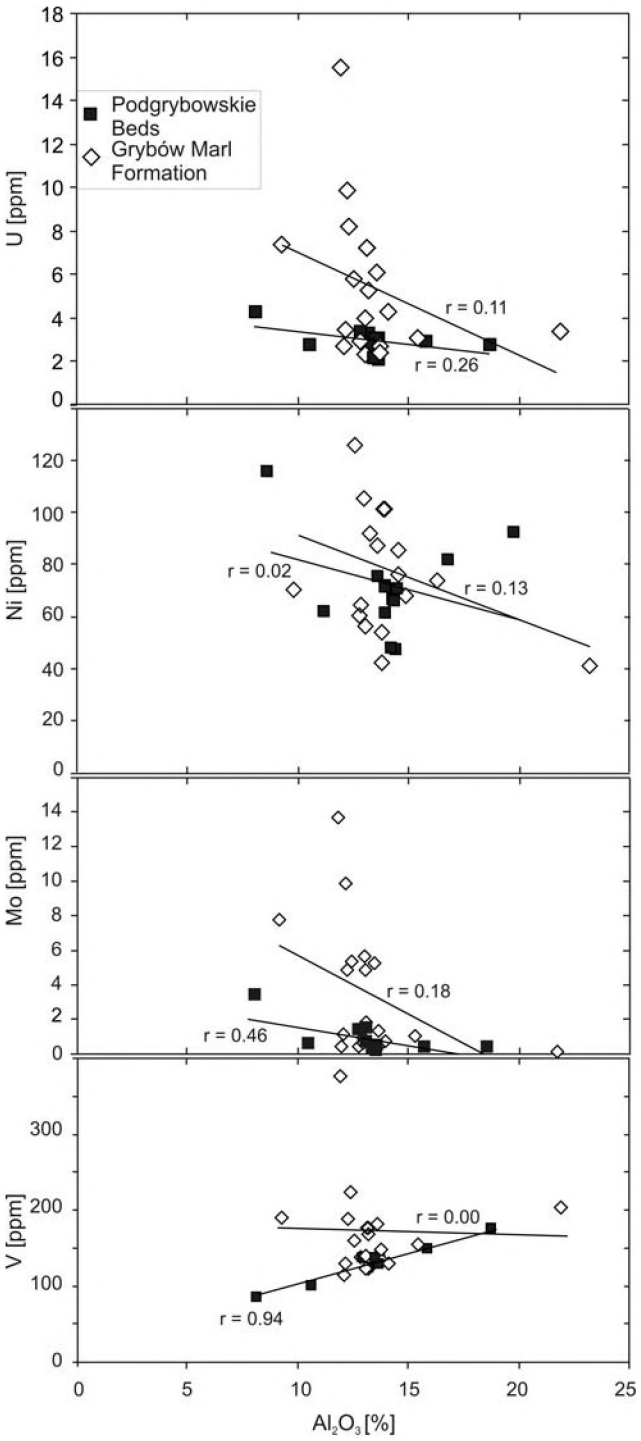

Fig. 9. Plot of the Grybów Succession samples within the RSTE *vs.* Al_2O_3 variation diagram.

Palaeoredox conditions

The RSTE concentrations in the sediments of the Grybów Unit studied are controlled by TOC and/or TS contents. The values of correlation coefficient vary from 0.69 to 0.89 (Tab. 2). An exception is Ni, the co-occurrence of which with TOC is insignificant (r = 0.22). Consequently, the dark grey and brown samples enriched in TOC and TS are also enriched in RSTE with a maximum in sample 16/05.

An authigenic uptake of U, Mo, V and Ni in sediments is facilitated by oxygen-depleted conditions. A catchment of RSTE from seawater may be accelerated by the formation of organometallic ligands in humic acids. Therefore, their concentrations frequently show a good correlation with the organic-carbon content in anoxic and non-sulphidic facies (Wignall and Maynard, 1993; Morford and Emerson, 1999; Algeo and Maynard, 2004; McManus *et al.*, 2005). Amounts of Mo and V correlated with TOC were recognized in the Oligocene–Miocene Maikop Series in the South Caspian Basin, where the overall higher trace metals content and TOC accumulation in the Rupelian, with a max-

Table 2

Pearson correlation matrix for redox-sensitive metals, TOC and TS in samples of the Grybów Unit (n = 30)

	U	V	Mo	Ni	TS	TOC	Al_2O_3
U	1.00						
V	0.84	1.00					
Mo	0.96	0.75	1.00				
Ni	0.58	0.38	0.62	1.00			
TS	0.88	0.72	0.89	0.77	1.00		
TOC	0.83	0.89	0.69	0.22	0.56	1.00	
Al_2O_3	-0.27	0.15	-0.37	-0.28	-0.40	-0.40	1.00

imum at the Rupelian–Chattian boundary, have been noted; geochemical proxies point to the dysoxic to anoxic conditions prevailing during the sedimentation of this series (Hudson *et al.*, 2008).

The onset of U enrichment requires less reducing conditions than those for Mo, thus U is taken up earlier during progressive burial and a gradual shift to more reducing conditions (Helz *et al.*, 1996; Algeo and Tribovillard, 2009). The highest values of Mo/U ratio in the upper part of the Grybów formation indicate more reducing conditions.

The concentration of U in the Grybów Unit brownish black shales can be explained by the uptake of U by authigenic U oxide (e.g., Tribovillard *et al.*, 2006). The positive correlation between U and TOC could be coincidental, as U oxides are precipitated and at the same time the preservation of organic matter is enhanced in anoxic conditions. The low U/Th ratios imply domination of an aerobic environment, episodically altered by dysoxic (samples 15/05, 19/05, 20/05) and anoxic (sample16/05) conditions. The threshold values of U/Th are 0.75 and 1.25 and values higher than these indicate dysoxic and anoxic conditions, respectively (cf. Jones and Manning, 1994).

The anoxic-sulphidic conditions must have developed in the sediments as is suggested by geochemical proxies, i.e. TOC/TS and V/(V+Ni) ratios. The V/(V+Ni) ratios of the studied samples range from 0.61 to 0.83 with one outlier at 0.42. V/(V+Ni) ratios extent from 0.46 to 0.6 and from 0.54 to 0.82 reflect dysoxic and anoxic conditions, respectively (cf. Lewan and Maynard, 1982; Hatch and Leventhal, 1992). Thus, the succession studied seems to indicate dysoxic to anoxic conditions.

If the TOC-TS relation is taken into consideration, samples 16/05 and 19/05 from the Grybów Marl Formation are classified as anoxic-euxinic. The Grybów Marl Formation shows a slight positive correlation of TOC with TS and a trend-line that follows the "normal marine" line. For the Podgrybowskie Beds, this correlation is negative. Therein, TOC contents are low, often due to dilution by detritus. The enhanced S concentration probably resulted from diagenetic pyritisation, confirmed by the pyrite morphology (framboids, crystals, and massive lumps; Wignall and Newton, 1998).

The most probable scenario of pyrite formation in the material studied involves pyritisation, which occurs in the anoxic sediments covered by an oxygenated water column. Pyrite formed in sediments is more variable in form and size than pyrite precipitated in the euxinic water column. The formation of pyrite nuclei at the chemocline positioned in the water column is limited by time and they occur as uniformly small (< 6 μm in diameter) framboids (Wilkin and Barnes, 1996). Framboidal aggregates settle on the sediment-water interface and pyrite growth is halted. Diagenetic pyrite can be texturally distinctive, occurring as large framboids, crystals, and massive lumps. Framboids that are variable in size are preferentially formed in the sediments near the redox transition (Wignall and Newton, 1998).

In summary, the Grybów Unit succession studied was deposited under oxygen-deficient conditions. The oxygen concentration/depletion was controlled by the turbiditic currents that could have ventilated the bottom waters. The upper part of the Grybów Marl Formation was developed as more pelagic sediments instead of turbiditic facies. Additionally, the Chełmski section displays more distal turbiditic facies (with Bouma intervals), which contain less detritus and lower numbers of reworked nannofossils. Contrary to that, the Górnikowski section represents more proximal turbiditic facies with Tab Bouma intervals (Oszczypko-Clowes, 2008; Oszczypko-Clowes *et al.*, 2015). However, Bojanowski (2007) proposed that the fine-grained Krosno succession represents proximal turbidite facies, deposited between submarine canyons, by way of which currents carried coarse-grained material to more distal and deeper parts of the basin.

Consequently, the upper part of the Grybów Formation of the Chełmski section records more anoxic-sulphidic conditions, while the Górnikowski section depicts dysoxic sediments with organic matter diluted by mineral detritus. Oxygen periodically available in the bottom waters also may have influenced on the sediments, causing downward migration of the oxic/anoxic front. This is seen fairly well in the pair of samples 19-20/05, which are succeeded by turbidites of the Krosno Beds. Samples 19/05 and 20/05 are in direct contact. The sample 20/05 is overlain by turbidite deposits (M. Oszczypko-Clowes pers. comm., 2016). Sample 19/05 contains higher concentrations of RSTE at lesser quantities of TOC than the underlying sample 20/05. It is possible that the trace elements went downward due to oxic/anoxic interface migration as a result of post-depositional reoxidation (Thomson *et al.*, 1993). In general, the downward migration of the reoxygenation front may have leached the RSTE and oxidized organic matter from the uppermost part of the sediments (sample 20/05). Then, RSTE were reprecipitated (sample 19/05) at the depth, where the redox front was halted. The organic matter originated from land plants, which were delivered by rivers. The photic zone concomitantly fed by nutrients was a location of occasionally enhanced bioproductivity.

CONCLUSIONS

The Oligocene Grybów succession in the Ropa Tectonic Window is represented by deep-sea, mainly turbidite sediments comprising a shaly-marly-sandstone sequence, including brownish black, fine-grained sediments. These

TOC-enriched sediments occur especially among more distal turbidite facies.

The terrestrial organic matter was transported to the basin by rivers. The liptinite and vitrinite macerals, kerogen type II/III and low $\delta^{13}C_{org.}$, indicate the land-plant contribution of the organic matter. Anoxic and sulphidic conditions within the sediments, evidenced by abundant and large-sized framboidal pyrite, the enrichment in RSTE, high ratios of U/Th and V/(V+Ni) (1.6 and 0.75, respectively), developed during deposition of the Grybów Formation.

In surface waters enriched in nutrients, phytoplankton bloomed effectively. This is recorded as the interbedding of more calcareous sediments. The presence of marine organic matter is inferred from the predominance of liptinite macerals (e.g., algal bituminite), kerogen type I/II and increasing values of $\delta^{13}C_{org.}$ (–25.2 ‰). The accumulation of reactive organic matter resulted in the rise of anoxia and acidification of the bottom waters. It is documented in the deposition of weakly calcareous black shales. Oxygen-deficient conditions are indicated by V/(V+Ni) and U/Th ratios (both ratios are 0.8).

At the same time, more proximal turbidite facies were deposited on the continental slope. The turbidity currents diluted the organic remains and ventilated the depositional environments, where anoxia occurred in the deeper sector of the basin. Therefore, anoxia did not reach the continental slope until sedimentation of the upper part of the Grybów Marl Formation.

Moreover, the transition from turbidites to hemipelagic sediments may have caused a non-steady state of the diagenetic environment in a shallow-burial setting. Consequently, post-depositional changes in RSTE concentrations occurred, owing to the downward migration of the oxic/anoxic front. The uppermost part of the Grybów Formation is an example of how the turbidity currents that gave rise to the Krosno Beds might have reduced the RSTE concentrations and then re-accumulated them deeper in the sediments.

Acknowledgements

The author acknowledges help from M. Oszczypko-Clowes with the collection of rock samples. Many thanks are extended to the Petrogeo Laboratory for Rock-Eval pyrolysis and the Laboratory of Isotope Geology and Geoecology (Wrocław University) for isotopic analysis. The author warmly thanks A. Uchman (Jagiellonian University) and F. Simpson (University of Windsor), who made helpful comments on the English version of the manuscript. Special thanks go to J. Soták and M. Bojanowski for their thorough reviews of this article, and to B. Budzyń and W. Mizerski for the editorial remarks. The research was undertaken as a part of a project of Polish Ministry of Science and Higher Education Grant No. N N307 531038.

REFERENCES

ACME Analytical Laboratories, Ltd, 2013. *AcmeLabs Schedule of Services and Fees* 2013. Vancouver, Canada. p. 14.

Algeo, T. J. & Maynard, J. B., 2004. Trace-element behavior and redox facies in core shales of Upper Pennsylvanian Kansas-type cyclothems. *Chemical geology*, 206, 3: 289–318.

Algeo, T. J. & Tribovillard, N., 2009. Environmental analysis of paleoceanographic systems based on molybdenum–uranium covariation. *Chemical Geology*, 268, 3: 211–225.

Asaro, F., Alvarez, L. W., Alvarez, W. & Michel, H. V., 1982. Geochemical anomalies near the Eocene/Oligocene and Permian/Triassic boundaries. *Geological Society of America Special Papers*, 190: 517–528.

Bechtel, A., Hámor-Vidó, M., Gratzer, R., Sachsenhofer, R. F. & Püttmann, W., 2012. Facies evolution and stratigraphic correlation in the early Oligocene Tard Clay of Hungary as revealed by maceral, biomarker and stable isotope composition. *Marine and Petroleum Geology*, 35: 55–74.

Berner, R. A. & Raiswell, R., 1983. Burial of organic carbon and pyrite sulfur ion sediments over Phanerozoic time: a new theory. *Geochimica et Cosmochimica Acta*, 47: 855–862.

Bieda, F., Geroch, S., Koszarski, L., Książkiewicz, M. & Żytko, K., 1963. Stratigraphie des Karpathes externes polonaises. *Biuletyn Instytutu Geologicznego*, 181: 5–174. [In French.]

Bojanowski, M. J., 2007. The onset of orogenic activity recorded in the Krosno shales from the Grybów unit (Polish Outer Carpathians). *Acta Geologica Polonica*, 57: 509–522.

Bojanowski, M. J., 2012. Geochemical paleogradient in pore waters controlled by AOM recorded in an Oligocene laminated limestone from the Outer Carpathians. *Chemical Geology*, 292–293: 45–56.

Coplen, T. B., Brand, W. A., Gehre, M., Gröning, M., Meijer, H. J., Toman, B. & Verkouteren, R. M., 2006. New guidelines for $\delta^{13}C$ measurements. *Analytical Chemistry*, 78: 2439–2441.

Coxall, H. K., Wilson, P. A., Pälike, H., Lear, C. H. & Backman, J., 2005. Rapid stepwise onset of Antarctic glaciation and deeper calcite compensation in the Pacific Ocean. *Nature*, 433: 53–57.

Diester-Haass, L., 1991. Eocene/Oligocene paleoceanography in the Antarctic Ocean, Atlantic sector (Maud Rise, ODP leg 113, site 689B and 690B). *Marine Geology*, 100: 249–276.

DeConto, R. M. & Pollard, D., 2003. Rapid Cenozoic glaciation of Antarctica induced by declining atmospheric CO_2. *Nature*, 421: 245–249.

Espitalié, J. & Bordenave, M. L., 1993. Screening techniques for source rock evaluation: tools for source rocks routine analysis: Rock-Eval pyrolysis. In: Bordenave, M. L. (ed.), *Applied Petroleum Geochemistry*. Technip, Paris, pp. 237–272.

Espitalié, J., Deroo, G. & Marquis, F., 1985. La pyrolyse Rock-Eval et ses applications. Première partie. *Oil & Gas Science and Technology - Revue de l'Institut Francais du Petrole*, 40: 563–579.

Hatch, J. R. & Leventhal, J. S., 1992. Relationship between inferred redox potential of the depositional environment and geochemistry of the Upper Pennsylvanian (Missourian) Stark Shale Member of the Dennis Limestone, Wabaunsee County, Kansas, USA. *Chemical Geology*, 99: 65–82.

Helz, G. R., Miller, C. V., Charnock, J. M., Mosselmans, J. F. W., Pattrick, R. A. D., Garner, C. D. & Vaughan, D. J., 1996. Mechanism of molybdenum removal from the sea and its concentration in black shales: EXAFS evidence. *Geochimica et Cosmochimica Acta*, 60, 19: 3631–3642.

Hudson, S. M., Johnson, C. L., Efendiyeva, M. A., Rowe, H. D., Feyzullayev, A. A. & Aliyev, C. S., 2008. Stratigraphy and geochemical characterization of the Oligocene–Miocene Maikop series: implications for the paleogeography of Eastern Azerbaijan. *Tectonophysics*, 451, 1: 40–55.

Jones, B. & Manning, D. A., 1994. Comparison of geochemical indices used for the interpretation of palaeoredox conditions in ancient mudstones. *Chemical Geology*, 111, 1: 111–129.

Kennett, J. P., 1977. Cenozoic evolution of Antarctic glaciation, the circum-Antarctic Ocean, and their impact on global paleoceanography. *Journal of Geophysical Research*, 82: 3843–3860.

Köster, J., Rospondek, M., Schouten, S., Kotarba, M., Zubrzycki, A. & Sinninghe Damste, J. S., 1998. Biomarker geochemistry of a foreland basin: Oligocene Menilite Formation in the Flysch Carpathians of Southeast Poland. *Organic Geochemistry*, 29, 649–669.

Kotarba, M. & Koltun, Y. V., 2006. Origin and habitat of hydrocarbons of the Polish and Ukrainian parts of the Carpathian Province. *AAPG Memoir*, 84: 395–443.

Kotlarczyk, J., Jerzmańska, A., Świdnicka, E. & Wiszniowska, T., 2006. A framework of ichthyofaunal ecostratigraphy of the Oligocene-Early Miocene strata of the Polish Outer Carpathian basin. *Annales Societatis Geologorum Poloniae*, 76: 1–111.

Kotlarczyk, J. & Uchman, A., 2012. Integrated ichnological and ichthyological analysis of oxygenation changes in the Menilite Formation during Oligocene, Skole and Subsilesian nappes, Polish Carpathians. *Palaeogeography, Palaeoclimatology, Palaeoecology*, 331–332: 104–118.

Kozikowski, H., 1956. Ropa-Pisarzowa unit, a new tectonic unit of the Polish flysch Carpathians. *Biuletyn Państwowego Instytutu Geologicznego*, 110: 93–137. [In Polish, with English summary.]

Krhovský, J., 1995. Early Oligocene palaeoenvironmental changes in the West Carpathian Flysch belt of Southern Moravia. In: *Proceedings of XV Congress of the Carpathian-Balkan Geological Association., September 1995. Geological Society of Greece, Special Publication*, 4: 209–213.

Książkiewicz, M., 1977. The Tectonics of the Carpathians. In: *Geology of Poland, vol. 4. Tectonics. The Alpine Tectonic Epoch.* Geological Institute, Warsaw, pp. 476– 608.

Leszczyński, S., 1997. Origin of the Sub-Menilite Globigerina Marl (Eocene–Oligocene transition) in the Polish Outer Carpathians. *Annales Societatis Geologorum Poloniae*, 67: 367–427.

Lewan, M. D. & Maynard, J. B., 1982. Factors controlling enrichment of vanadium and nickel in the bitumen of organic sedimentary rocks. *Geochimica et Cosmochimica Acta*, 46, 12: 2547–2560.

Lexa, J., Bezak, V., Elecko, M., Mello, J., Polak, M., Potfaj, M. & Vozar, J., 2000. *Geological Map of Western Carpathians and Adjacent Areas, 1:500,000.* Geological Survey of the Slovak Republic, Bratislava.

Liu, Z., Pagani, M., Zinniker, D., DeConto, R., Huber, M., Brinkhuis, H., Shah, S. R., Leckie, R. M. & Pearson, A., 2009. Global cooling during the Eocene-Oligocene climate transition. *Science*, 323, 5918: 1187–1190.

McManus, J., Berelson, W. M., Klinkhammer, G. P., Hammond, D. E. & Holm, C., 2005. Authigenic uranium: relationship to oxygen penetration depth and organic carbon rain. *Geochimica et Cosmochimica Acta*, 69, 1: 95–108.

Meyers, P. A., 1994. Preservation of elemental and isotopic source identification of sedimentary organic matter. *Chemical Geology*, 114: 289–302.

Morford, J. L. & Emerson, S., 1999. The geochemistry of redox sensitive trace metals in sediments. *Geochimica et Cosmochimica Acta*, 63: 1735–1750.

Olszewska, B., 1983. A contribution of the knowledge of planktonic foraminifers of the Globigerina Submenilite Marls of the Polish Outer Carpathians. *Kwartalnik Geologiczny*, 27: 546–570. [In Polish, with English summary.]

Oszczypko, N. & Oszczypko-Clowes, M., 2011. Stratigraphy and tectonics of the Świątkowa Wielka Tectonic Window (Magura Nappe, Polis Outer Carpathians). *Geologica Carpathica*, 62: 139–154.

Oszczypko-Clowes, M., 2008. The stratigraphy of the Oligocene deposits from the Ropa tectonic window (Grybów Nappe, Western Carpathians, Poland). *Geological Quarterly*, 52: 127–142.

Oszczypko-Clowes, M. & Oszczypko, N., 2004. The position and age of the youngest deposits in the Mszana Dolna and Szczawa tectonic windows (Magura Nappe, Western Carpathians, Poland). *Acta Geologica Polonica*, 54: 339–367.

Oszczypko-Clowes, M. & Ślączka, A., 2006. Nannofossil biostratigraphy of the Oligocene deposits in the Grybów tectonic window (Grybów Unit, Western Carpathians, Poland). *Geologica Carpathica*, 57: 473–482.

Oszczypko-Clowes, M., Wójcik-Tabol, P. & Płoszaj, M., 2015. Source areas of the Grybów sub-basin: micropaleontological, mineralogical and geochemical provenance analysis (Outer Western Carpathians, Poland). *Geologica Carpathica*, 66: 515–534.

Pagani, M., Zachos, J. C., Freeman, K. H., Tipple, B., & Bohaty, S., 2005. Marked decline in atmospheric carbon dioxide concentrations during the Paleogene. *Science*, 309, 5734: 600–603.

Peters, K. E. & Moldowan, J. M., 1993. *The Biomarker Guide, Interpreting Molecular Fossils in Petroleum and Ancient Sediments.* Prentice Hall. Englewood Cliffs, NJ United States, 363 pp.

Popov, S. V., Rögl, F., Rozanov, A. Y., Steininger, F. F., Shcherba, I. G. & Kovač, M., 2004. Lithological–Paleogeographic maps of Paratethys – 10 maps Late Eocene to Pliocene. *Courier Forschungsinstitut Senckenberg*, 250: 1–46.

Prothero, D. R., 1994. *The Eocene-Oligocene Transition: Paradise Lost.* Columbia University Press, New York, 291 pp.

Puglisi, D., Badescu, D., Carbone, S., Corso, S., Franchi, R., Gigliuto, L. G., Loiacono, F., Miclaus, C. & Moretti, E., 2006. Stratigraphy, petrography and palaeogeographic significance of the Early Oligocene "menilite facies" of the Tarcau Nappe (Eastern Carpathians, Romania). *Acta Geologica Polonica*, 56, 1: 105–120.

Raiswell, R., & Berner, R. A., 1985. Pyrite formation in euxinic and semi-euxinic sediments. *American Journal of Science*, 285: 710–724.

Rospondek, M. J., Köster, J., & Damsté, J. S., 1997. Novel C_{26} highly branched isoprenoid thiophenes and alkane from the Menilite Formation, Outer Carpathians, SE Poland. *Organic Geochemistry*, 26: 295–304.

Sachsenhofer, R. F. & Schulz, H.-M., 2006. Architecture of Lower Oligocene source rocks in the Alpine Foreland Basin: a model for syn- and postdepositional source rock features in the Paratethyan Realm. *Petroleum Geoscience*, 12: 363–377.

Sachsenhofer, R. F., Stummer, B., Georgiev, G., Dellmour, R., Bechtel, A., Gratzer, R. & Coric, S., 2009. Depositional environment and hydrocarbon source potential of the Oligocene Ruslar Formation (Kamchia Depression; western Black Sea). *Marine and Petroleum Geology*, 26: 57–84.

Sarkar, A., Sarangi, S., Bhattacharya, S. K. & Ray, A. K., 2003a. Carbon isotopes across the Eocene-Oligocene boundary sequence of Kutch, western India: Implications to oceanic productivity and pCO_2 change. *Geophysical Research Letters*, 30: 1–4.

Sarkar, A., Sarangi, S., Ebihara, M., Bhattacharya, S. K. & Ray, A. K., 2003b. Carbonate geochemistry across the Eocene/Oligocene boundary of Kutch, western India: implications to oceanic O_2-poor condition and foraminiferal extinction. *Chemical Geology*, 201, 3: 281–293.

Schulz, H. M., Sachsenhofer, R. F., Bechtel, A., Polesny, H., & Wagner, L., 2002. The origin of hydrocarbon source rocks in the Austrian Molasse Basin (Eocene–Oligocene transition). *Marine and Petroleum Geology*, 19: 683–709.

Schulz, H. M., Bechtel, A. & Sachsenhofer, R. F., 2005. The birth of the Paratethys during the Early Oligocene: From Tethys to an ancient Black Sea analogue? *Global and Planetary Change*, 49: 163–176.

Sikora, W., 1960. On the stratigraphy of the series in the tectonic window at Ropa near Gorlice (Western Carpathians). *Kwartalnik Geologiczny*, 4: 152–170. [In Polish, with English summary.]

Sikora, W., 1970. Geology of the Magura Nappe between Szymark Ruski and Nawojowa. *Biuletyn Instytutu Geologicznego*, 235: 5–121. [In Polish, with English summary.]

Skrzypek, G. & Jędrysek, M. O., 2005. $^{13}C/^{12}C$ ratio in peat cores: Record of past climates. In: Lichtfouse, E., Schwarzbauer, J. & Robert, D. (eds), *Environmental Chemistry - Green Chemistry and Pollutants in Ecosystems*. Springer Berlin Heidelberg, pp. 65–73.

Soták, J., 2008. Paleoenvironmental changes of the Carpathian Flysch Sea during the transition from the Peri-Tethyan to Black Sea-type basins. Mineralia Slovaca, 40: 253–254.

Soták, J., 2010. Paleoenvironmental changes across the Eocene-Oligocene boundary: insights from the Central-Carpathian Paleogene Basin. *Geologica Carpathica*, 61: 1–26.

Soták, J., Pereszlenyi, M., Marschalko, R., Milicka, J., & Starek, D., 2001. Sedimentology and hydrocarbon habitat of the submarine-fan deposits of the Central Carpathian Paleogene Basin (NE Slovakia). *Marine and Petroleum Geology*, 18: 87–114.

Ślączka, A., 1973. Wycieczka 1: Grybów-Polany-Berest-Krzyżówka. Punkt 1-4. In: Gucik, S., Ślączka, A. & Żytko, K. (eds), *Przewodnik geologiczny po wschodnich Karpatach fliszowych*. Wydawnictwa Geologiczne, Warszawa, pp. 78–87. [In Polish.]

Świdziński, H., 1963. Excursion B-I-1: Ciężkowice-Grybów-Krosno-Iwonicz Zdrój. In: Wdowiarz, S. & Nowak, W. (eds), *Association Géologique Karpato-Balkanique, VI-eme Congrès, Varsovie-Cracovie, Guide des Excursions: Karpates Externes*. Wydawnictwa Geologiczne, Warszawa, pp. 85–91.

Thomson, J., Higgs, N. C., Croudace, I. W., Colley, S. & Hydes, D. J., 1993. Redox zonation of elements at an oxic/post-oxic boundary in deep-sea sediments. *Geochimica et Cosmochimica Acta*, 57: 579–595.

Tribovillard, N., Algeo, T., Lyons, T. W. & Riboulleau, A., 2006. Trace metals as paleoredox and paleoproductivity proxies: an update. *Chemical Geology*, 232: 12–32.

Vetö, I., 1987. An Oligocene sink for organic carbon: upwelling in the Paratethys? *Palaeogeography, Palaeoclimatology, Palaeoecology*, 60: 143–153.

Vetö, I. & Hetényi, M., 1991. Fate of organic carbon and reduced sulphur in dysoxic-anoxic Oligocene facies of the Central Paratethys (Carpathian Mountains and Hungary). *Geological Society, Special Publications, London*, 58, 1: 449–460.

Wedepohl, K. H., 1971. Environmental influences on the chemical composition of shales and clays. In: Ahrens, L. H., Press, F., Runcorn, S. K. & Urey, H. C. (eds), *Physics and Chemistry of the Earth*. Pergamon, Oxford, pp. 307–331.

Więcław, D., 2002. *Origin of Oligocene oils from the Polish Flysch Carpathians: Organic sulfur in the kerogen of the Menilite shales and kinetics of hydrocarbon generation process*. Unpublished Ph. D. thesis, AGH University of Science and Technology, Kraków, pp. 131. [In Polish.]

Wignall, P. B. & Maynard, J. R., 1993. The sequence stratigraphy of transgressive black shales. *Source Rocks in a Sequence stratigraphic framework*, 37: 35–47.

Wignall, P. B. & Newton, R., 1998. Pyrite framboid diameter as a measure of oxygen deficiency in ancient mudrocks. *American Journal of Science*, 298: 537–552.

Wilkin, R. T. & Barnes, H. L., 1996. Pyrite formation by reactions of iron monosulfides with dissolved inorganic and organic sulfur species. *Geochimica et Cosmochimica Acta*, 60, 21: 4167–4179.

Wójcik-Tabol, P., 2015. Depositional redox conditions of the Grybów Succession (Oligocene, Polish Carpathians) in the light of petrological and geochemical indices. *Geological Quarterly*, 59: 603–614.

Zachos, J. C., Lohmann, K. C., Walker, J. C. & Wise, S. W., 1993. Abrupt climate change and transient climates during the Paleogene: A marine perspective. *The Journal of Geology*, pp. 191–213.

Zachos, J. C., Quinn, T. M. & Salamy, K. A., 1996. High-resolution (10^4 yr) deep-sea foraminiferal stable isotope records of the Eocene–Oligocene climate transition. *Paleoceanography*, 11: 251–266.